This article was downloaded by:
On: *23 January 2011*
Access details: *Access Details: Free Access*
Publisher *Taylor & Francis*
Informa Ltd Registered in England and Wales Registered Number: 1072954 Registered office: Mortimer House, 37-41 Mortimer Street, London W1T 3JH, UK

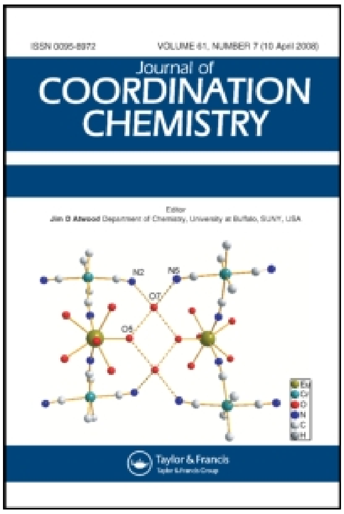

Journal of Coordination Chemistry

Publication details, including instructions for authors and subscription information:
http://www.informaworld.com/smpp/title~content=t713455674

Syntheses and structural determinations of the nine-coordinate rare earth metal: $Na_4[Dy^{III}(dtpa)(H_2O)]_2\cdot16H_2O$, $Na[Dy^{III}(edta)(H_2O)_3]\cdot3.25H_2O$ and $Na_3[Dy^{III}(nta)_2(H_2O)]\cdot5.5H_2O$

Jun Wang[a]; Guangrui Gao[a]; Zhaohong Zhang[b]; Xiangdong Zhang[a]; Yingjie Wang[a]
[a] Department of Chemistry, Liaoning University, Shenyang 110036, P. R. China [b] Department of Environment, Liaoning University, Shenyang 110036, P. R. China

First published on: 18 June 2007

To cite this Article Wang, Jun , Gao, Guangrui , Zhang, Zhaohong , Zhang, Xiangdong and Wang, Yingjie(2007) 'Syntheses and structural determinations of the nine-coordinate rare earth metal: $Na_4[Dy^{III}(dtpa)(H_2O)]_2\cdot16H_2O$, $Na[Dy^{III}(edta)(H_2O)_3]\cdot3.25H_2O$ and $Na_3[Dy^{III}(nta)_2(H_2O)]\cdot5.5H_2O$', Journal of Coordination Chemistry, 60: 20, 2221 — 2241, First published on: 18 June 2007 (iFirst)

To link to this Article: DOI: 10.1080/00958970701258622

URL: http://dx.doi.org/10.1080/00958970701258622

PLEASE SCROLL DOWN FOR ARTICLE

Full terms and conditions of use: http://www.informaworld.com/terms-and-conditions-of-access.pdf

This article may be used for research, teaching and private study purposes. Any substantial or systematic reproduction, re-distribution, re-selling, loan or sub-licensing, systematic supply or distribution in any form to anyone is expressly forbidden.

The publisher does not give any warranty express or implied or make any representation that the contents will be complete or accurate or up to date. The accuracy of any instructions, formulae and drug doses should be independently verified with primary sources. The publisher shall not be liable for any loss, actions, claims, proceedings, demand or costs or damages whatsoever or howsoever caused arising directly or indirectly in connection with or arising out of the use of this material.

Journal of Coordination Chemistry
Vol. 60, No. 20, 15 October 2007, 2221–2241

Taylor & Francis
Taylor & Francis Group

Syntheses and structural determinations of the nine-coordinate rare earth metal: $Na_4[Dy^{III}(dtpa)(H_2O)]_2 \cdot 16H_2O$, $Na[Dy^{III}(edta)(H_2O)_3] \cdot 3.25H_2O$ and $Na_3[Dy^{III}(nta)_2(H_2O)] \cdot 5.5H_2O$

JUN WANG*†, GUANGRUI GAO†, ZHAOHONG ZHANG‡,
XIANGDONG ZHANG† and YINGJIE WANG†

†Department of Chemistry, Liaoning University, Shenyang 110036, P. R. China
‡Department of Environment, Liaoning University, Shenyang 110036, P. R. China

(*Received 29 August 2006; in final form 1 September 2006*)

Three complexes, $Na_4[Dy^{III}(dtpa)(H_2O)]_2 \cdot 16H_2O$, $Na[Dy^{III}(edta)(H_2O)_3] \cdot 3.25H_2O$ and $Na_3[Dy^{III}\ (nta)_2(H_2O)] \cdot 5.5H_2O$, have been synthesized in aqueous solution and characterized by FT–IR, elemental analyses, TG–DTA and single-crystal X-ray diffraction. $Na_4[Dy^{III}(dtpa)(H_2O)]_2 \cdot 16H_2O$ crystallizes in the monoclinic system with $P2_1/n$ space group, $a = 18.158(10)$ Å, $b = 14.968(9)$ Å, $c = 20.769(12)$ Å, $\beta = 108.552(9)^\circ$, $V = 5351(5)$ Å^3, $Z = 4$, $M = 1517.87\ \mathrm{g\,mol^{-1}}$, $D_c = 1.879\ \mathrm{g\,cm^{-3}}$, $\mu = 2.914\ \mathrm{mm^{-1}}$, $F(000) = 3032$, and its structure is refined to $R_1(F) = 0.0500$ for 9384 observed reflections $[I > 2\sigma(I)]$. $Na[Dy^{III}(edta)(H_2O)_3] \cdot 3.25H_2O$ crystallizes in the orthorhombic system with $Fdd2$ space group, $a = 19.338(7)$ Å, $b = 35.378(13)$ Å, $c = 12.137(5)$ Å, $\beta = 90^\circ$, $V = 8303(5)$ Å^3, $Z = 16$, $M = 586.31\ \mathrm{g\,mol^{-1}}$, $D_c = 1.876\ \mathrm{g\,cm^{-3}}$, $\mu = 3.690\ \mathrm{mm^{-1}}$, $F(000) = 4632$, and its structure is refined to $R_1(F) = 0.0307$ for 4027 observed reflections $[I > 2\sigma(I)]$. $Na_3[Dy^{III}(nta)_2(H_2O)] \cdot 5.5H_2O$ crystallizes in the orthorhombic system with $Pccn$ space group, $a = 15.964(12)$ Å, $b = 19.665(15)$ Å, $c = 14.552(11)$ Å, $\beta = 90^\circ$, $V = 4568(6)$ Å^3, $Z = 8$, $M = 724.81\ \mathrm{g\,mol^{-1}}$, $D_c = 2.102\ \mathrm{g\,cm^{-3}}$, $\mu = 3.422\ \mathrm{mm^{-1}}$, $F(000) = 2848$, and its structure is refined to $R_1(F) = 0.0449$ for 4033 observed reflections $[I > 2\sigma(I)]$. The coordination polyhedra are tricapped trigonal prism for $Na_4[Dy^{III}(dtpa)(H_2O)]_2 \cdot 16H_2O$ and $Na_3[Dy^{III}(nta)_2(H_2O)] \cdot 5.5H_2O$, but monocapped square antiprism for $Na[Dy^{III}(edta)(H_2O)_3] \cdot 3.25H_2O$. The crystal structures of these three complexes are completely different from one another. The three-dimensional geometries of three polymers are 3-D layer-shaped structure for $Na_4[Dy^{III}(dtpa)(H_2O)]_2 \cdot 16H_2O$, 1-D zigzag type structure for $Na[Dy^{III}(edta)(H_2O)_3] \cdot 3.25H_2O$ and a 2-D parallelogram for $Na_3[Dy^{III}(nta)_2(H_2O)] \cdot 5.5H_2O$. According to thermal analyses, the collapsing temperatures are 356°C for $Na_4[Dy^{III}(dtpa)(H_2O)]_2 \cdot 16H_2O$, 371°C for $Na[Dy^{III}(edta)(H_2O)_3] \cdot 3.25H_2O$ and 387°C for $Na_3[Dy^{III}(nta)_2(H_2O)] \cdot 5.5H_2O$, which indicates that their crystal structures are very stable.

Keywords: DyIII; Dtpa (diethylenetriamine-*N*,*N*,*N*′,N″,*N*″-pentaacetic acid); Edta (ethylenediamine-*N*,*N*,*N*′,*N*′-tetraacetic acid); Nta (= nitrilotriacetic acid); Structure

---

*Corresponding author. Email: wangjun890@126.com

Journal of Coordination Chemistry
ISSN 0095-8972 print/ISSN 1029-0389 online © 2007 Taylor & Francis
DOI: 10.1080/00958970701258622

1. Introduction

Progress has been achieved in the coordination chemistry of rare earth metal (RE) complexes with various aminopolycarboxylic acid ligands, which are of interest in applications for different purposes, and in the research and development of new materials [1]. In medicinal and biochemistry, RE complexes are widely investigated for: (1) high-spin paramagnetism and the ability to enhance the longitudinal relaxation rate of water protons, Gd-dtpa complexes have been used as contract agents in magnetic resonance imaging (MRI) [2–6], (2) because some RE ions have desirable radioactive characteristics, their corresponding complexes become excellent candidates for radiation synovectomy and radioimmunotherapy, e.g. ^{153}Sm, ^{165}Dy, ^{166}Ho, and ^{177}Lu complexes [7–9], (3) special photophysical properties of RE complexes as luminescent labels in various fluoroimmunoassays [10] and (4) hydrolysis of DNA and RNA with high specificity [11–18]. Research on their crystal and molecular structures is very important to determine their behavior *in vivo*. For example, the coordination number, the presence of coordination water and the formation of polynuclear species can dramatically change the value of these complexes.

In a given oxidation state, the crystal and molecular structures of RE complexes with aminopolycarboxylic acid ligands depend on the radius of central metal ions and the nature of counter cation(s). For the potassium salts of RE-dtpa complexes, difference in ionic radius not only influences the coordination number, but also the molecular structure. The RE-dtpa complexes, whose central metal ions are ahead of the Dy^{III} ion (including the Dy^{III} ion) in the order of RE ions, possess mononuclear structures, such as $K_2[Eu^{III}(dtpa)(H_2O)]\cdot 6H_2O$, $K_2[Gd^{III}(dtpa)(H_2O)]\cdot 6H_2O$, $K_2[Dy^{III}(dtpa)(H_2O)]\cdot 6H_2O$ [19] and $K_2[Y^{III}(dtpa)(H_2O)]\cdot 7H_2O$ [20]. As for the RE ions behind the Dy^{III} ion, their dtpa complexes are binuclear, ($K_4[Ho^{III}{}_2(dtpa)_2]\cdot 4H_2O$ [19], $K_4[Er_2^{III}(dtpa)_2]\cdot 7H_2O$ and $K_4[Yb_2^{III}(dtpa)_2]\cdot 8H_2O$). Hence, Dy^{III} is regarded as the division between mononuclear structure and binuclear structure for their potassium salts. There is generally similarity between the potassium and sodium salts of RE complexes with aminopolycarboxylic acid ligands. As a result, $Na_4[Dy^{III}(dtpa)(H_2O)]_2\cdot 16H_2O$ is mononuclear. In the $Na_4[Dy^{III}(dtpa)(H_2O)]_2\cdot 16H_2O$, there are two kinds of coordination moieties, which are connected by six types of bridging coordination modes. In order to analyze the influence of ligand species on crystal and molecular structures, the $Na[Dy^{III}(edta)(H_2O)_3]\cdot 3.25H_2O$ and $Na_3[Dy^{III}(nta)_2(H_2O)]\cdot 5.5H_2O$ were also synthesized. Scheme 1 exhibits the structures of three aminopolycarboxylic acid ligands.

2. Experimental

2.1. *Syntheses of complexes*

2.1.1. Syntheses of $Na_4[Dy^{III}(dtpa)(H_2O)]_2\cdot 16H_2O$. The $Na_4[Dy^{III}(dtpa)(H_2O)]_2\cdot 16H_2O$ was prepared by mixing Dy_2O_3 (0.9325 g, 2.5 mmol) and H_5dtpa (1.9668 g, 5 mmol) in 100 mL water (molar ratio of Dy^{III} to dtpa is 1 : 1). The mixed solution was heated under stirring and refluxing. After 6 h the solution became transparent, and then the pH was adjusted to 6.5 by dropping dilute $NaHCO_3$ aqueous solution. The resulting solution was concentrated to 20 mL, and colorless crystals of Dy^{III}

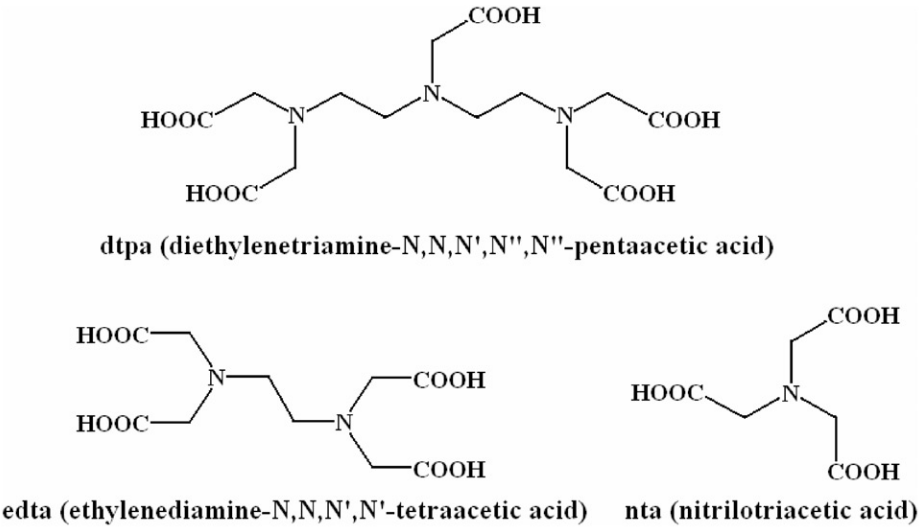

dtpa (diethylenetriamine-N,N,N',N'',N''-pentaacetic acid)

edta (ethylenediamine-N,N,N',N'-tetraacetic acid) nta (nitrilotriacetic acid)

Scheme 1. The structures of three kinds of aminopolycarboxylic acid ligands.

complex was obtained after two weeks at room temperature. The elemental analyses for C, H and N were carried out on a Perkin–Elmer 240 instrument. The contents of Dy^{III} ion were measured by edta titration after microwave digestion. Anal. Found (%): Dy 21.44, C 22.19, H 4.76, N 5.53; Calcd (%): Dy 21.41, C 22.16, H 4.78, N 5.54. The formula ($C_{28}H_{72}Dy_2N_6O_{38}Na_4$) is consistent with the diffraction analysis.

2.1.2. Syntheses of $Na[Dy^{III}(edta)(H_2O)_3] \cdot 3.25H_2O$. Colorless crystals of $Na[Dy^{III}(edta)(H_2O)_3] \cdot 3.25H_2O$ were prepared by mixing Dy_2O_3 (0.9325 g, 2.5 mmol) and H_4edta (1.4612 g, 5 mmol) in an analogous manner. Anal. Found (%): Dy 27.75, C 20.51, H 4.20, N 4.76; Calcd (%): Dy 27.72, C 20.49, H 4.21, N 4.78. This formula ($C_{10}H_{24.5}DyN_2O_{14.25}Na$) is consistent with the result of diffraction analysis.

2.1.3. Syntheses of $Na_3[Dy^{III}(nta)_2(H_2O)] \cdot 5.5H_2O$. Colorless crystals of $Na_3[Dy^{III}(nta)_2(H_2O)] \cdot 5.5H_2O$ were prepared by mixing Dy_2O_3 (0.9325 g, 2.5 mmol) and H_3nta (1.9114 g, 10.0 mmol) powders and following the same procedure. Anal. Found (%): Dy 22.44, C 19.91, H 3.47, N 3.84; Calcd (%): Dy 22.42, C 19.89, H 3.48, N 3.86. This formula ($C_{12}H_{25}DyN_2O_{18.5}Na_3$) is consistent with the result of diffraction analysis.

2.2. *Determination of FT–IR spectra*

The FT–IR spectra of $Na_4[Dy^{III}(dtpa)(H_2O)]_2 \cdot 16H_2O$, $Na[Dy^{III}(edta)(H_2O)_3] \cdot 3.25H_2O$ and $Na_3[Dy^{III}(nta)_2(H_2O)] \cdot 5.5H_2O$, and corresponding ligands, H_5dpta, H_4edta and H_3nta, were determined by a Perkin–Elmer Spectrum One FT–IR spectrometer. All the results are given in figure 1.

2.3. *Determination of TG–DTA*

Thermal analyses were determined by Mettler–Toledo 851^e thermogravimetric analyzer under N_2 ($20\,mL\,min^{-1}$) from room temperature to 800°C at a heating rate of $10^{\circ}C\,min^{-1}$. The results are given in figure 2.

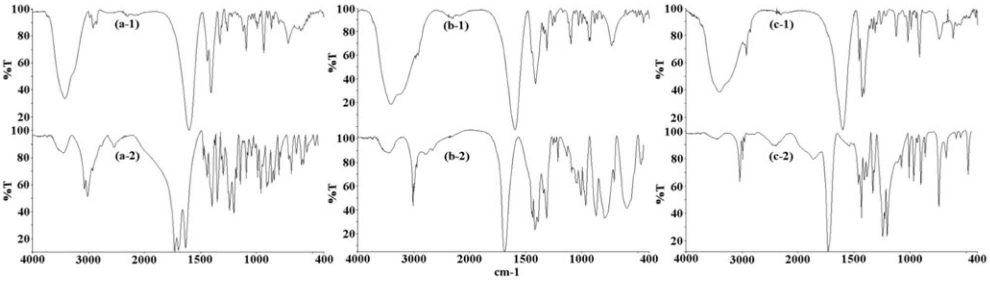

Figure 1. FT–IR spectra of three title complexes and their corresponding ligands. (a-1) $Na_4[Dy^{III}(dtpa)(H_2O)]_2 \cdot 16H_2O$; (b-1) $Na[Dy^{III}(edta)(H_2O)_3] \cdot 3.25H_2O$; (c-1) $Na_3[Dy^{III}(nta)_2(H_2O)] \cdot 5.5H_2O$; (a-2) H_5; dtpa; (b-2) H_4edta; (c-2) H_3nta.

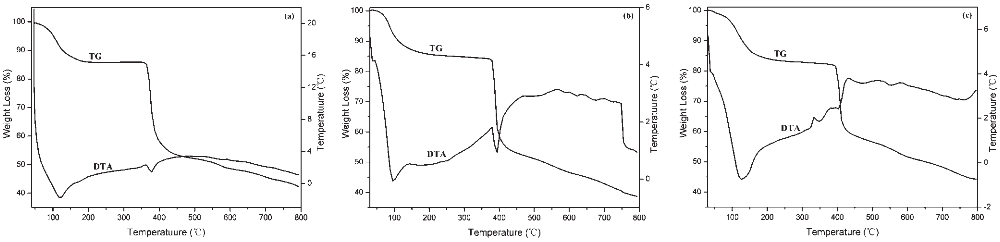

Figure 2. TG–DTA of three title complexes. (a) $Na_4[Dy^{III}(dtpa)(H_2O)]_2 \cdot 16H_2O$; (b) $Na[Dy^{III}(edta)(H_2O)_3] \cdot 3.25H_2O$; (c) $Na_3[Dy^{III}(nta)_2(H_2O)] \cdot 5.5H_2O$.

2.4. *X-ray diffraction of single crystals*

Data on the title complexes were collected on a Bruker SMART CCD type X-ray diffractometer system with graphite-monochromatized Mo-Kα radiation ($\lambda = 0.71073$ Å). The structures were solved by direct methods. All non-hydrogen atoms were refined anisotropically by full-matrix least-squares methods. All calculations were performed by the SHELXL-97 program on PDP11/44 and Pentium MMX/166 computers. The details of crystal data collection and refinement parameters for the $Na_4[Dy^{III}(dtpa)(H_2O)]_2 \cdot 16H_2O$, $Na[Dy^{III}(edta)(H_2O)_3] \cdot 3.25H_2O$ and $Na_3[Dy^{III}(nta)_2(H_2O)] \cdot 5.5H_2O$ are listed in table 1. Selected bond lengths and angles are listed in tables 2–4, respectively. For comparison, the crystal data of some RE complexes similar to $Na_4[Dy^{III}(dtpa)(H_2O)]_2 \cdot 16H_2O$, $Na[Dy^{III}(edta)(H_2O)_3] \cdot 3.25H_2O$ and $Na_3[Dy^{III}(nta)_2(H_2O)] \cdot 5.5H_2O$ are also listed in tables 5–7.

3. Results and discussion

3.1. *FT–IR spectra*

Comparisons between the FT–IR spectra of ligands and corresponding complexes reveal changes due to complexation.

As shown in figure 1(a-1) and (a-2), the ν(C–N) of $Na_4[Dy^{III}(dtpa)(H_2O)]_2 \cdot 16H_2O$ is at 1092 cm^{-1}, red-shifted 54 cm^{-1} compared to H_5dtpa (1146 cm^{-1}), indicating that the nitrogen atoms of H_5dtpa have coordinated to Dy^{III}. The ν_{as}(COOH) of H_5dpta at 1733 cm^{-1} disappears in the FT–IR spectrum of $Na_4[Dy^{III}(dtpa)(H_2O)]_2 \cdot 16H_2O$; the

Table 1. Crystal data and structure refinement for three title complexes.

Complex	$Na_4[Dy^{III}(dtpa)(H_2O)]_2 \cdot 16H_2O$	$Na[Dy^{III}(edta)(H_2O)_3] \cdot 3.25H_2O$	$Na_3[Dy^{III}(nta)_2(H_2O)] \cdot 5.5H_2O$
Empirical formula	$C_{28}H_{72}Dy_2N_6O_{38}Na_4$	$C_{10}H_{24.5}DyN_2O_{14.25}Na$	$C_{12}H_{25}DyN_2O_{18.5}Na_3$
Formula weight	1517.86	586.30	724.80
T (K)	293(2)	293(2)	293(2)
λ (Mo-Kα) (Å)	0.71073	0.71073	0.71073
Crystal system	Monoclinic	Orthorhombic	Orthorhombic
Space group	$P2_1/n$	$Fdd2$	$Pccn$
a (Å)	18.158(10)	19.338(7)	15.964(12)
b (Å)	14.968(9)	35.378(13)	19.665(15)
c (Å)	20.769(12)	12.137(5)	14.552(11)
β (°)	108.552(9)	90	90
Volume (Å^3)	5351(5)	8303(5)	4568(6)
Z	4	16	8
D_{Calcd} (Mg m^{-3})	1.879	1.876	2.102
Absorption coefficient (mm^{-1})	2.914	3.690	3.422
$F(000)$	3032	4632	2848
Crystal size (mm^3)	$0.22 \times 0.20 \times 0.18$	$0.32 \times 0.20 \times 0.16$	$0.28 \times 0.24 \times 0.20$
θ range for data collection (°)	2.44–25.01	2.06–26.34	1.64–25.01
Index ranges	$-19 \le h \le 21$, $-17 \le k \le 11$, $-24 \le l \le 24$	$-22 \le h \le 22$, $-27 \le k \le 44$, $-14 \le l \le 15$	$-18 \le h \le 18$, $-11 \le k \le 23$, $-16 \le l \le 17$
Reflections collected	26910	10038	22013
Independent reflections	9384 [R(int) = 0.0732]	4027 [R(int) = 0.0356]	4033 [R(int) = 0.0741]
Completeness to θ_{max} (%)	99.4	97.3	100.0
Max. and min. transmission	1.000000 and 0.684552	1.000000 and 0.715700	1.000000 and 0.544943
Data/restraints/parameters	9384/0/703	4027/1/271	4033/0/334
Goodness of fit on F^2	0.958	1.041	1.046
Final R indices [$I > 2\sigma(I)$]*	$R_1(F) = 0.0500$, $wR_2\ (F^2) = 0.1005$	$R_1(F) = 0.0307$, $wR_2\ (F^2) = 0.0799$	$R_1(F) = 0.0449$, $wR_2\ (F^2) = 0.0991$
R indices (all data)	$R_1(F) = 0.0817$, $wR_2\ (F^2) = 0.1111$	$R_1(F) = 0.0375$, $wR_2\ (F^2) = 0.0827$	$R_1(F) = 0.0699$, $wR_2\ (F^2) = 0.1157$
Largest diff. peak and hole (e Å^{-3})	1.130 and −1.375	0.891 and −0.509	1.911 and −2.341
Absorption correction	Semi-empirical from equivalents	Semi-empirical from equivalents	Semi-empirical from equivalents
Refinement method	Full-matrix least-squares on F^2	Full-matrix least-squares on F^2	Full-matrix least-squares on F^2

*$R_1(F) = \Sigma\ \|F_o| - |F_c\|/\Sigma\ |F_o|$ and $wR_2(F^2) = \{\Sigma[w(F_o^2 - F_c^2)^2]/\Sigma\ w(F_o^2)^2\}^{1/2}$.

Table 2. Selected bond lengths (Å) and angles (°) for $Na_4[Dy^{III}(dtpa)(H_2O)]_2 \cdot 16H_2O$ (only in the coordination polyhedron).[a]

Dy(1)–O(1)	2.351(5)	Dy(1)–N(1)	2.605(7)	Dy(2)–O(18)	2.419(5)
Dy(1)–O(3)	2.395(5)	Dy(1)–N(2)	2.562(7)	Dy(2)–O(20)	2.363(5)
Dy(1)–O(5)	2.364(6)	Dy(1)–N(3)	2.693(6)	Dy(2)–O(22)	2.495(5)
Dy(1)–O(7)	2.345(5)	Dy(2)–O(12)	2.395(5)	Dy(2)–N(4)	2.685(6)
Dy(1)–O(9)	2.334(6)	Dy(2)–O(14)	2.333(6)	Dy(2)–N(5)	2.558(6)
Dy(1)–O(11)	2.536(6)	Dy(2)–O(16)	2.324(5)	Dy(2)–N(6)	2.596(7)

O(1)–Dy(1)–O(3)	93.32(19)	O(7)–Dy(1)–N(1)	68.3(2)	O(18)–Dy(2)–O(20)	93.55(19)
O(1)–Dy(1)–O(5)	149.42(19)	O(7)–Dy(1)–N(2)	83.2(2)	O(18)–Dy(2)–O(22)	70.46(18)
O(1)–Dy(1)–O(7)	75.65(19)	O(7)–Dy(1)–N(3)	64.3(2)	O(20)–Dy(2)–O(22)	74.41(18)
O(1)–Dy(1)–O(9)	87.6(2)	O(9)–Dy(1)–N(1)	146.4(2)	O(12)–Dy(2)–N(4)	63.05(19)
O(1)–Dy(1)–O(11)	73.01(19)	O(9)–Dy(1)–N(2)	131.1(2)	O(12)–Dy(2)–N(5)	131.1(2)
O(3)–Dy(1)–O(5)	72.74(19)	O(9)–Dy(1)–N(3)	63.3(2)	O(12)–Dy(2)–N(6)	145.62(19)
O(3)–Dy(1)–O(7)	133.97(19)	O(11)–Dy(1)–N(1)	116.33(19)	O(14)–Dy(2)–N(4)	64.86(19)
O(3)–Dy(1)–O(9)	138.19(19)	O(11)–Dy(1)–N(2)	135.4(2)	O(14)–Dy(2)–N(5)	85.0(2)
O(3)–Dy(1)–O(11)	70.43(18)	O(11)–Dy(1)–N(3)	124.3(2)	O(14)–Dy(2)–N(6)	67.9(2)
O(5)–Dy(1)–O(7)	133.48(19)	N(1)–Dy(1)–N(2)	69.8(2)	O(16)–Dy(2)–N(4)	70.93(19)
O(5)–Dy(1)–O(9)	85.6(2)	N(1)–Dy(1)–N(3)	119.4(2)	O(16)–Dy(2)–N(5)	68.72(19)
O(5)–Dy(1)–O(11)	76.65(19)	N(2)–Dy(1)–N(3)	69.2(2)	O(16)–Dy(2)–N(6)	129.60(19)
O(7)–Dy(1)–O(9)	86.7(2)	O(12)–Dy(2)–O(14)	85.8(2)	O(18)–Dy(2)–N(4)	134.94(19)
O(7)–Dy(1)–O(11)	141.28(19)	O(12)–Dy(2)–O(16)	84.58(19)	O(18)–Dy(2)–N(5)	72.14(19)
O(9)–Dy(1)–O(11)	69.96(19)	O(12)–Dy(2)–O(18)	139.23(19)	O(18)–Dy(2)–N(6)	66.64(18)
O(1)–Dy(1)–N(1)	65.2(2)	O(12)–Dy(2)–O(20)	87.6(2)	O(20)–Dy(2)–N(4)	130.60(19)
O(1)–Dy(1)–N(2)	134.7(2)	O(12)–Dy(2)–O(22)	70.68(18)	O(20)–Dy(2)–N(5)	135.1(2)
O(1)–Dy(1)–N(3)	130.6(2)	O(14)–Dy(2)–O(16)	134.23(19)	O(20)–Dy(2)–N(6)	65.0(2)
O(3)–Dy(1)–N(1)	66.59(19)	O(14)–Dy(2)–O(18)	133.70(19)	O(22)–Dy(2)–N(4)	123.68(18)
O(3)–Dy(1)–N(2)	73.4(2)	O(14)–Dy(2)–O(20)	74.81(19)	O(22)–Dy(2)–N(5)	133.22(18)
O(3)–Dy(1)–N(3)	135.32(19)	O(14)–Dy(2)–O(22)	141.72(19)	O(22)–Dy(2)–N(6)	117.11(19)
O(5)–Dy(1)–N(1)	127.8(2)	O(16)–Dy(2)–O(18)	73.74(19)	N(4)–Dy(2)–N(5)	69.6(2)
O(5)–Dy(1)–N(2)	68.3(2)	O(16)–Dy(2)–O(20)	148.89(19)	N(4)–Dy(2)–N(6)	119.2(2)
O(5)–Dy(1)–N(3)	71.3(2)	O(16)–Dy(2)–O(22)	74.58(18)	N(5)–Dy(2)–N(6)	70.4(2)

[a] Symmetry transformations used to generate equivalent atoms: #1 $-x+1.5$, $y+0.5$, $-z+0.5$; #2 $-x+0.5$, $y+0.5$, $-z+0.5$; #3 $-x+1$, $-y+2$, $-z$; #4 $-x+0.5$, $y-0.5$, $-z+0.5$; #5 $-x+1.5$, $y-0.5$, $-z+0.5$.

Table 3. Selected bond lengths (Å) and angles (°) for $Na[Dy^{III}(edta)(H_2O)_3] \cdot 3.25H_2O$ (only in the coordination polyhedron).[a]

Dy(1)–O(1)	2.349(5)	Dy(1)–O(7)	2.408(5)	Dy(1)–O(11)	2.390(5)
Dy(1)–O(3)	2.403(5)	Dy(1)–O(9)	2.533(4)	Dy(1)–N(1)	2.625(5)
Dy(1)–O(5)	2.362(5)	Dy(1)–O(10)	2.457(5)	Dy(1)–N(2)	2.673(6)

O(1)–Dy(1)–O(3)	71.65(18)	O(5)–Dy(1)–O(9)	74.16(17)	O(3)–Dy(1)–N(2)	114.34(18)
O(1)–Dy(1)–O(5)	78.69(19)	O(5)–Dy(1)–O(10)	142.43(18)	O(5)–Dy(1)–N(1)	78.06(19)
O(1)–Dy(1)–O(7)	141.37(18)	O(5)–Dy(1)–O(11)	77.89(19)	O(5)–Dy(1)–N(2)	65.54(18)
O(1)–Dy(1)–O(9)	67.99(17)	O(7)–Dy(1)–O(9)	138.65(17)	O(7)–Dy(1)–N(1)	89.75(17)
O(1)–Dy(1)–O(10)	104.95(19)	O(7)–Dy(1)–O(10)	70.97(17)	O(7)–Dy(1)–N(2)	63.61(17)
O(1)–Dy(1)–O(11)	137.50(18)	O(7)–Dy(1)–O(11)	79.92(19)	O(9)–Dy(1)–N(1)	131.25(17)
O(3)–Dy(1)–O(5)	140.46(18)	O(9)–Dy(1)–O(10)	72.97(17)	O(9)–Dy(1)–N(2)	129.60(18)
O(3)–Dy(1)–O(7)	70.67(17)	O(9)–Dy(1)–O(11)	71.73(19)	O(10)–Dy(1)–N(1)	138.61(19)
O(3)–Dy(1)–O(9)	115.97(17)	O(10)–Dy(1)–O(11)	74.95(16)	O(10)–Dy(1)–N(2)	126.80(18)
O(3)–Dy(1)–O(10)	72.12(17)	O(1)–Dy(1)–N(1)	67.80(19)	O(11)–Dy(1)–N(1)	138.8(2)
O(3)–Dy(1)–O(11)	141.34(18)	O(1)–Dy(1)–N(2)	127.71(19)	O(11)–Dy(1)–N(2)	71.3(2)
O(5)–Dy(1)–O(7)	128.66(17)	O(3)–Dy(1)–N(1)	66.9(2)	N(1)–Dy(1)–N(2)	68.4(2)

[a] Symmetry transformations used to generate equivalent atoms: #1 $x+0.25$, $-y+0.25$, $z+0.25$; #2 $x-0.25$, $-y+0.25$, $z-0.25$.

Table 4. Selected bond lengths (Å) and angles (°) for $Na_3[Dy^{III}(nta)_2(H_2O)] \cdot 5.5H_2Om$ (only in the coordination polyhedron).[a]

Dy(1)–O(1)	2.360(6)	Dy(1)–O(7)	2.385(6)	Dy(1)–O(13)	2.501(6)
Dy(1)–O(3)	2.365(7)	Dy(1)–O(9)	2.345(6)	Dy(1)–N(1)	2.606(7)
Dy(1)–O(5)	2.336(6)	Dy(1)–O(11)	2.367(6)	Dy(1)–N(2)	2.619(7)
O(1)–Dy(1)–O(3)	86.6(2)	O(5)–Dy(1)–O(9)	140.4(2)	O(3)–Dy(1)–N(2)	136.4(2)
O(1)–Dy(1)–O(5)	130.0(2)	O(5)–Dy(1)–O(11)	82.5(2)	O(5)–Dy(1)–N(1)	66.2(2)
O(1)–Dy(1)–O(7)	144.2(2)	O(5)–Dy(1)–O(13)	135.1(2)	O(5)–Dy(1)–N(2)	74.3(2)
O(1)–Dy(1)–O(9)	76.3(2)	O(7)–Dy(1)–O(9)	96.6(2)	O(7)–Dy(1)–N(1)	134.8(2)
O(1)–Dy(1)–O(11)	81.5(2)	O(7)–Dy(1)–O(11)	130.2(2)	O(7)–Dy(1)–N(2)	65.1(2)
O(1)–Dy(1)–O(13)	77.3(2)	O(7)–Dy(1)–O(13)	67.3(2)	O(9)–Dy(1)–N(1)	128.5(2)
O(3)–Dy(1)–O(5)	75.7(2)	O(9)–Dy(1)–O(11)	72.0(2)	O(9)–Dy(1)–N(2)	67.8(2)
O(3)–Dy(1)–O(7)	77.9(2)	O(9)–Dy(1)–O(13)	72.2(2)	O(11)–Dy(1)–N(1)	71.2(2)
O(3)–Dy(1)–O(9)	142.0(2)	O(11)–Dy(1)–O(13)	141.7(2)	O(11)–Dy(1)–N(2)	65.8(2)
O(3)–Dy(1)–O(11)	139.1(2)	O(1)–Dy(1)–N(1)	63.8(2)	O(13)–Dy(1)–N(1)	124.2(2)
O(3)–Dy(1)–O(13)	71.0(2)	O(1)–Dy(1)–N(2)	137.1(2)	O(13)–Dy(1)–N(2)	111.6(2)
O(5)–Dy(1)–O(7)	77.1(2)	O(3)–Dy(1)–N(1)	68.4(2)	N(1)–Dy(1)–N(2)	124.1(2)

[a] Symmetry transformations used to generate equivalent atoms #1 $x-0.5, -y+1, -z+1.5$; #2 $-x+0.5, y, z+0.5$; #3 $-x, -y+1, -z+2$; #4 $-x, -y+1, -z+1$; #5 $-x+0.5, y, z-0.5$; #6 $x+0.5, -y+1, -z+1.5$; #7 $-x+0.5, -y+1.5, z$.

Table 5. The crystal data of Dy-dtpa complexes with different counter cations.

Complex	Structure	Crystal system	Space group	Conformation of coordination polyhedron	Reference
$Na_4[Dy^{III}(dtpa)(H_2O)]_2 \cdot 16H_2O$	Mononuclear	Monoclinic	$P2_1/n$	Monocapped square antiprism	–
$K_2[Dy^{III}(dtpa)(H_2O)] \cdot 6H_2O$	Mononuclear	Triclinic	$P\bar{1}$	Monocapped square antiprism	[25]
$Cs_4[Dy^{III}_2(dtpa)_2(H_2O)] \cdot 13H_2O$	Binuclear	Monoclinic	$C2/c$	Monocapped square antiprism	[26]
$(NH_4)_2[Dy^{III}_2(dtpa)_2] \cdot 4H_2O$	Binuclear	Triclinic	$P\bar{1}$	Tricapped trigonal prism	[24]

Table 6. The crystal data of Dy-edta complexes with different counter cations.

Complex	Coordination number	Crystal system	Space group	Conformation of coordination polyhedron	Reference
$Na[Dy^{III}(edta)(H_2O)_3] \cdot 3.25H_2O$	9	Orthorhombic	$Fdd2$	Monocapped square antiprism	–
$K[Dy^{III}(edta)(H_2O)_3] \cdot 3.5H_2O$	9	Orthorhombic	$Fdd2$	Monocapped square antiprism	–
$Cs[Dy^{III}(edta) (H_2O)_2] \cdot 3H_2O$	8	Monoclinic	$P2_1/c$	Monocapped square antiprism	[28]

$\nu_{as}(COO)$ of $Na_4[Dy^{III}(dtpa)(H_2O)]_2 \cdot 16H_2O$ is at $1603\,cm^{-1}$ red-shifted $32\,cm^{-1}$ compared to H_5dtpa ($1635\,cm^{-1}$); the $\nu_s(COO)$ of $Na_4[Dy^{III}(dtpa)(H_2O)]_2 \cdot 16H_2O$ is at $1409\,cm^{-1}$, blue-shifted $12\,cm^{-1}$ compared to H_5dtpa ($1397\,cm^{-1}$). These changes confirm that oxygen from the carboxyl groups coordinate to Dy^{III} [21]. There is a broad $\nu(OH)$ band of H_2O near $3422\,cm^{-1}$ revealing the presence of H_2O.

As shown in figure 1(b-1) and (b-2), the $\nu(C–N)$ of $Na[Dy^{III}(edta)(H_2O)_3] \cdot 3.25H_2O$ is at $1097\,cm^{-1}$, red-shifted $37\,cm^{-1}$ compared to H_4edta ($1134\,cm^{-1}$), indicating that

Table 7. The crystal data of Dy-nta complexes with different counter cations.

Complex	Coordination number	Crystal system	Space group	Conformation of coordination polyhedron	Reference
$Na_3[Dy^{III}(nta)_2(H_2O)] \cdot 5.5H_2O$	9	Orthorhombic	*Pccn*	Monocapped square antiprism	–
$K_3[Dy^{III}(nta)_2(H_2O)] \cdot 5H_2O$	9	Monoclinic	*C2/c*	Tricapped trigonal prism	[30]
$(NH_4)_3[Dy^{III}(nta)_2]$	8	Monoclinic	*C2/c*	Dicapped trigonal antiprism	[30]

nitrogen atoms of H_4edta coordinate to Dy^{III}. The $\nu_{as}(COO)$ of $Na[Dy^{III}(edta)(H_2O)_3] \cdot 3.25H_2O$ at $1598\,cm^{-1}$ is red-shifted $96\,cm^{-1}$ compared to H_4edta ($1694\,cm^{-1}$); the $\nu_s(COO)$ of $Na[Dy^{III}(edta)(H_2O)_3] \cdot 3.25H_2O$ is at $1414\,cm^{-1}$, blue-shifted $23\,cm^{-1}$ compared to H_4edta ($1391\,cm^{-1}$), confirming that oxygen from the carboxyl groups coordinate Dy^{III}. There is a broad $\nu(OH)$ band of H_2O near $3418\,cm^{-1}$ revealing the presence of H_2O in the complex molecule.

As shown in figure 1(c-1) and (c-2), the $\nu(C–N)$ of $Na_3[Dy^{III}(nta)_2(H_2O)] \cdot 5.5H_2O$ is at $1125\,cm^{-1}$ is red-shifted $81\,cm^{-1}$ compared with H_3nta ($1206\,cm^{-1}$), indicating nitrogen of H_3nta coordinate to Dy^{III}. The $\nu_{as}(COO)$ of $Na_3[Dy^{III}(nta)_2(H_2O)] \cdot 5.5H_2O$ is at $1602\,cm^{-1}$, red-shifted $131\,cm^{-1}$ compared to H_3nta ($1733\,cm^{-1}$); the $\nu_s(COO)$ of $Na_3[Dy^{III}(nta)_2(H_2O)] \cdot 5.5H_2O$ is at $1412\,cm^{-1}$, blue-shifted $27\,cm^{-1}$ compared with H_3nta ($1385\,cm^{-1}$), confirming that oxygen from the carboxyl groups coordinate to Dy^{III}. There is a broad $\nu(OH)$ band of H_2O near $3421\,cm^{-1}$ revealing the presence of H_2O in the complex molecule.

3.2. *Thermal analyses*

The thermal decomposition of the title complexes was studied using TG–DTA. As shown in figure 2, the TG curves exhibit a typical three-stage decomposition pattern. Corresponding to the weight loss of each stage, there are obvious endothermic peaks in the DTA curves.

As shown in figure 2(a), for $Na_4[Dy^{III}(dtpa)(H_2O)]_2 \cdot 16H_2O$ the first stage weight loss starting from room temperature to 198°C corresponds to the expulsion of crystal water molecules. The weight loss ratio is about 14%. Corresponding to the first stage weight loss, there is a marked endothermic peak in the DTA curve (117°C). From 198 to 356°C, there is little weight loss, which means that the crystal structure is stable until 356°C. The second stage weight loss of 33% is attributed to decomposition starting from 356 to 467°C. There is also a marked endothermic peak in the DTA curve (379°C). The third stage weight loss from decompositions of carboxylate, 467 to 794°C, is about 11%. The total weight loss ratio is about 58% according to the mass loss calculation. It is estimated that the remainder is a $Na_2CO_3–Dy_2O_3–Dy_2(CO_3)_3$ mixture.

As shown in figure 2(b), the first stage weight loss for $Na[Dy(edta)(H_2O)_3] \cdot 3.25H_2O$ from room temperature to 198°C corresponds to the expulsion of crystal water molecules. The weight loss ratio is about 14%. Corresponding to the weight loss of the first stage, there is a marked endothermic peak in the DTA curve (95°C). From 198 to 371°C, the weight loss ratio is only about 2%, indicating that the crystal structure is very stable, and did not collapse until 371°C. The second stage weight loss from decomposition of complex from 371 to 458°C is about 31%. There is also a marked endothermic peak in the DTA curve (394°C). The third stage weight loss from decompositions of carboxylate from 458 to 794°C is about 14%. The total weight loss ratio is about 61% according to the mass loss calculation. It is estimated that the remainder is a Na_2O–Dy_2O_3 mixture.

As shown in figure 2(c), the first stage weight loss for $Na_3[Dy(nta)_2(H_2O)] \cdot 5.5H_2O$ from room temperature to 198°C corresponds to the expulsion of crystal water. The weight loss ratio is about 16%. Corresponding to the weight loss of first stage, there is a marked endothermic peak in the DTA curve (126°C). During the temperature range of 198–387°C, the weight loss is only about 2%, indicating the crystal is very stable. At 348°C, there was not a weight loss in the TG curve but there was an obvious endothermic process in the DTA curve, which means that the sample melted. The second stage weight loss decomposition of complex, from 387–459°C, is about 24%. There is also an endothermic peak in the DTA curve (403°C). The third stage weight loss from the decompositions of carboxylate (459–795°C) is about 14%. In the corresponding section of DTA curve, there is not an obvious endothermic process. The total weight loss ratio is about 56% according to the mass loss calculation. It is estimated that the remainder is Na_2CO_3–Na_2O–Dy_2O_3 mixture.

3.3. *Molecular and crystal structures*

3.3.1. Molecular and crystal structures of $Na_4[Dy^{III}(dtpa)(H_2O)]_2 \cdot 16H_2O$. As shown in figure 3, each Dy^{III} ion is nine-coordinated. Generally, for binuclear RE complexes, two central metal ions are in similar coordination environments. However, there are many differences in bond lengths and angles between the two moieties of $Na_4[Dy^{III}(dtpa)(H_2O)]_2 \cdot 16H_2O$, which is similar to $K[KLa(Httha)(H_2O)] \cdot 8H_2O$ [22]. Hence, there

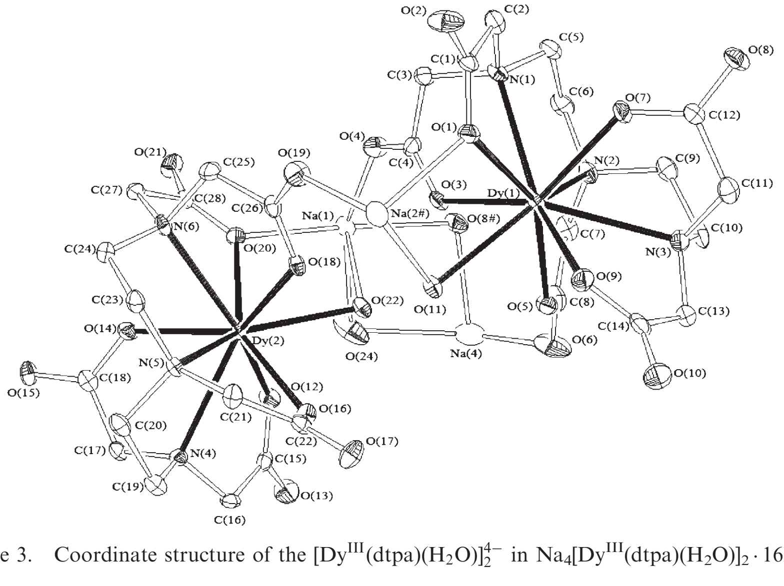

Figure 3. Coordinate structure of the $[Dy^{III}(dtpa)(H_2O)]_2^{4-}$ in $Na_4[Dy^{III}(dtpa)(H_2O)]_2 \cdot 16H_2O$.

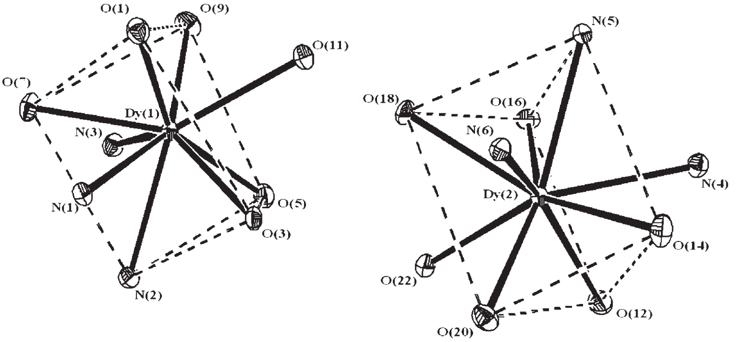

Figure 4. Coordinating polyhedrons around the Dy^{III} ions in $Na_4[Dy^{III}(dtpa)(H_2O)]_2 \cdot 16H_2O$.

are two different moieties, Moiety(1) and Moiety(2), in $Na_4[Dy^{III}(dtpa)(H_2O)]_2 \cdot 16H_2O$, the two central metal ions of which are labeled as Dy(1) and Dy(2), respectively.

Dy(1) and Dy(2) are both coordinated by one oxygen from one water, three amine nitrogen atoms and five carboxyl oxygen atoms from one dtpa ligand. The average bond length of Dy(1)–O is the same as that of Dy(2)–O (2.388(5) Å), whereas, the average bond length of Dy(1)–N (2.620(7) Å) is a little longer than that of Dy(2)–N (2.613(6) Å). In general, Dy–O bonds are more stable than Dy–N bonds.

According to Muetterties and Guggenbergers' definition for nine-coordinate complexes [23], two idealized polyhedra should be C_{4v} monocapped square antiprism and D_{3h} tricapped trigonal prism. The torsion angle of the bottom plane is important to judge which conformation the polyhedron adopts. It is the dihedral angle between two trigonal planes, which is 0° for C_{4v} monocapped square antiprism, but 26.4° for D_{3h} tricapped trigonal prism. As shown in figure 4, the torsion angle is 24.26° between N(3)–O(7)–N(2) and N(1)–O(7)–N(2), and 22.85° between N(4)–O(14)–N(5) and N(6)–O(14)–N(5). They are both near 26.4°, so it is considered that the coordination polyhedra both adopt the pseudo D_{3h} tricapped trigonal prismatic conformation, similar to other RE complexes with dtpa, such as $(NH_4)_2[Dy^{III}(dtpa)] \cdot 4H_2O$, $(NH_4)_2[Ho^{III}(dtpa)] \cdot 4H_2O$, $(NH_4)_2[Er^{III}(dtpa)] \cdot 4H_2O$ and $(NH_4)_2[Yb^{III}(dtpa)] \cdot 4H_2O$ [25]. Taking the coordination polyhedron around Dy(1) for example, the top plane is composed of O(1), O(7) and O(9), and the bottom plane is composed of O(3), N(2) and O(5), constituting a trigonal prism approximately. Out of profiles, three capping positions are occupied by N(1), N(3) and O(11), respectively. The Dy^{III} ion and three capping atoms are coplanar. The coordination polyhedron around Dy(2) is similar.

Four Dy-dtpa complexes synthesized previously are listed in table 5. The radius of counter cation is an important factor for the coordinate structure. The radii of NH_4^+ and Cs^+ are relatively big, and take up more space than Na^+ and K^+ in the crystal lattices. It is possible to make the coordination anions closer and to become binuclear.

The radius of counter cation also influences the coordinating polyhedron. For example, in the complex $K_2[Dy^{III}(dtpa)(H_2O)] \cdot 6H_2O$, the bond angles of $\angle O(1)Dy(1)O(11)$, $\angle O(3)Dy(1)O(11)$, $\angle O(5)Dy(1)O(11)$ and $\angle O(9)Dy(1)O(11)$ range from 68.40(11)° to 80.16(11)°. However, the corresponding four angles of $Na_4[Dy^{III}(dtpa)(H_2O)]_2 \cdot 16H_2O$ range from 69.96(19)° to 76.65(19)°. The range is smaller than that of $K_2[Dy^{III}(dtpa)(H_2O)] \cdot 6H_2O$ because the radius of K^+ is bigger than that of Na^+ distorting the coordination polyhedra more than Na^+.

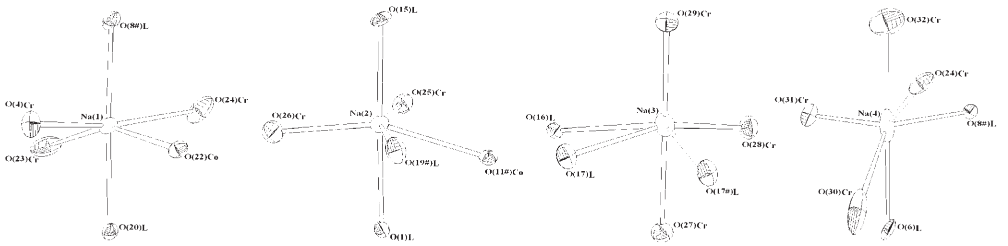

Figure 5. Coordinate structures of the Na ion in $Na_4[Dy^{III}(dtpa)(H_2O)]_2 \cdot 16H_2O$. L: the oxygen atom comes from the dtpa ligand; Cr: the oxygen atom comes from the crystal water molecule; Co: the oxygen atom comes from the coordination water molecule.

The $Na_4[Dy^{III}(dtpa)(H_2O)]_2 \cdot 16H_2O$ crystallizes in the monoclinic system with $P2_1/n$ space group. In the crystal lattices, there are four kinds of sodium ions, Na(1), Na(2), Na(3) and Na(4), with coordination number six. As shown in figure 5, each sodium atom is coordinated by six oxygen atoms with different sources. The bond lengths of Na–O range from 2.293(9) Å to 2.835(11) Å, and the average bond length is 2.472(8) Å. The Na ions connect complex moieties yielding the 3-D layer-shaped structure.

As shown in figure 6, there are six types of bridging coordination modes in the $Na_4[Dy^{III}(dtpa)(H_2O)]_2 \cdot 16H_2O$, each of which is provided with the distinct crystal engineering functions. Modes I, II and III depict the connecting modes between the same complex moieties. They could be called "5+5", because the two extremities of the chain are both five-member rings. Modes A, B and C describe the connecting modes between Moiety(1) and (2), belonging to "5+4" mode, because one extremity is a five-member ring, and the other is a four-member ring.

Figure 7 exhibits a zigzag type building block. Moiety (1) and Moiety (2) are connected with the Mode B yielding a $Na_4[Dy^{III}(dtpa)(H_2O)]_2 \cdot 16H_2O$ molecule, so Mode B is considered as the innermolecular connecting mode. The distance between Dy(1) and Dy(2) (6.430(8) Å) is short compared with those of other connecting modes; two Moiety(2)s from the different $Na_4[Dy^{III}(dtpa)(H_2O)]_2 \cdot 16H_2O$ molecules are connected with the Mode II yielding the zigzag type building block.

Figure 8 exhibits how six zigzag type building blocks arrange in a unit cell. Two parallel "edges" of zigzag type building block, which are just two $Na_4[Dy^{III}(dtpa)(H_2O)]_2 \cdot 16H_2O$ molecules, belong to the different layers.

As shown in figure 9, there are four $Na_4[Dy^{III}(dtpa)(H_2O)]_2 \cdot 16H_2O$ molecules in a layer, connected with Modes A, C, Modes I and III. These connecting modes are considered as the innerlayer connecting modes.

In figure 10, the bevel edges of zigzag type building blocks, Mode II, connect the different layers, so Mode II is considered as an interlayer connecting mode. The distance between Dy(2) and Dy(2#) (11.223(5) Å) is the longest in those of all the connecting modes.

Figure 11 shows the 3-D structure of the crystal of $Na_4[Dy^{III}(dtpa)(H_2O)]_2 \cdot 16H_2O$. The layer-shaped structure in a unit cell extend around yielding 2-D network, and then bevel edges of the zigzag type building blocks act as the stanchions between 2-D networks yielding the 3-D layer-shaped structure. In a unit cell, there are many intermolecular hydrogen bonds, which make the 3-D layer-shaped structure more stable.

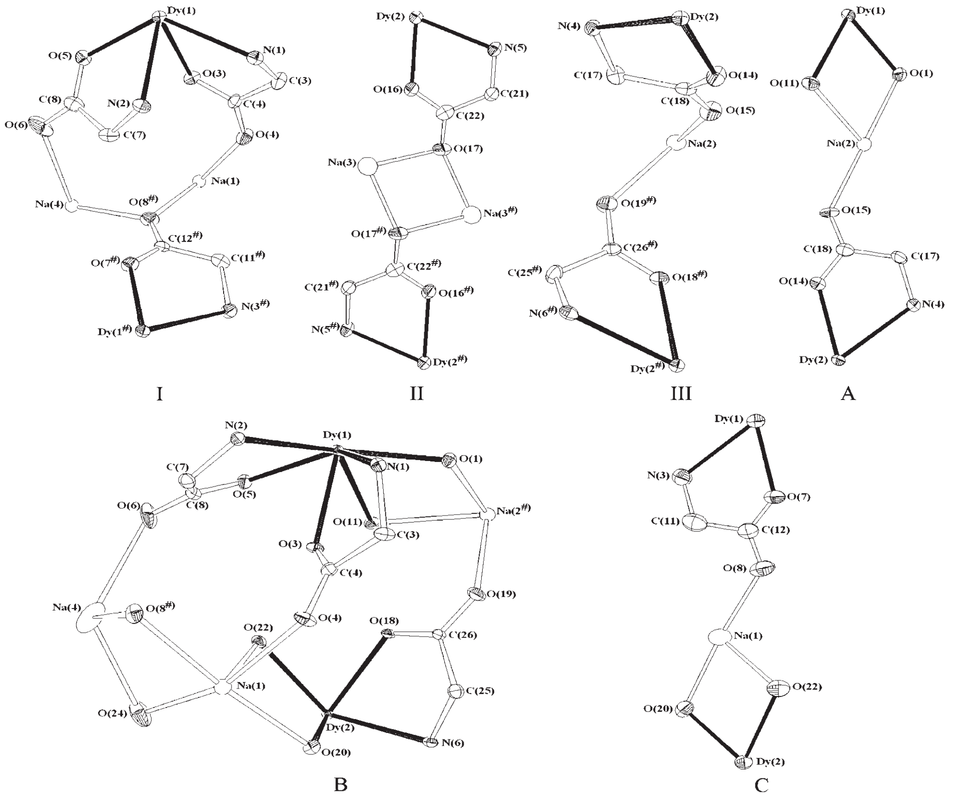

Figure 6. The different connecting modes of the Dy^{III} ions in a unit cell of $Na_4[Dy^{III}(dtpa)(H_2O)]_2 \cdot 16H_2O$. I: Dy(1)–8.210(2) Å–Dy(1); II: Dy(2)–11.223(5) Å–Dy(2); III: Dy(2)–8.251(3) Å–Dy(2); A: Dy(1)–10.407(5) Å–Dy(2); B: Dy(1)–6.430(8) Å–Dy(2); C: Dy(1)–10.296(4) Å–Dy(2).

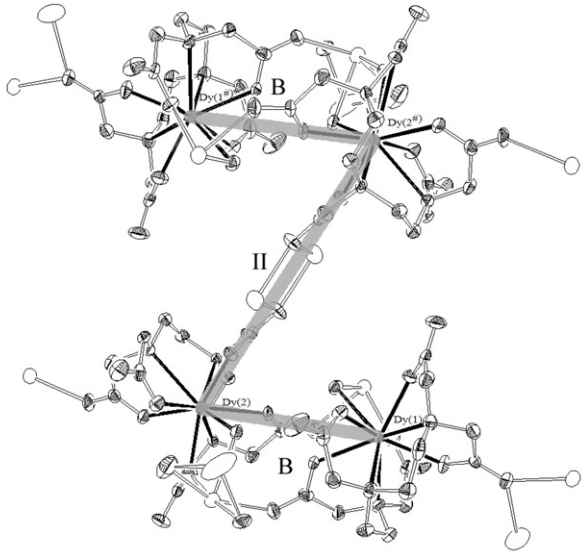

Figure 7. A zigzag type building block in a unit cell of $Na_4[Dy^{III}(dtpa)(H_2O)]_2 \cdot 16H_2O$.

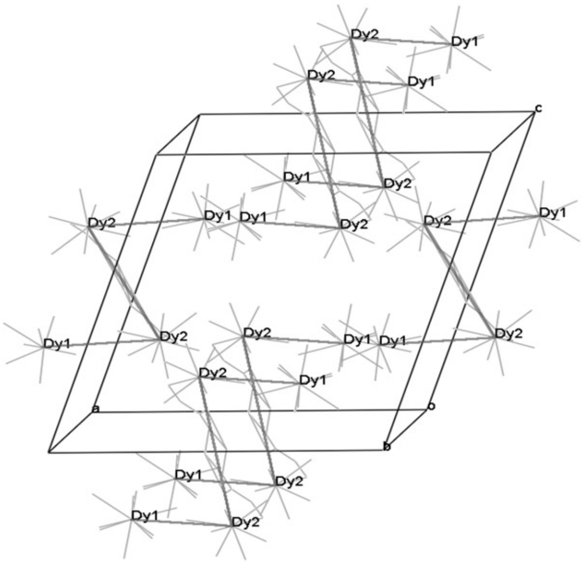

Figure 8. Arrangement of the zigzag type building blocks in a unit cell of $Na_4[Dy^{III}(dtpa)(H_2O)]_2 \cdot 16H_2O$.

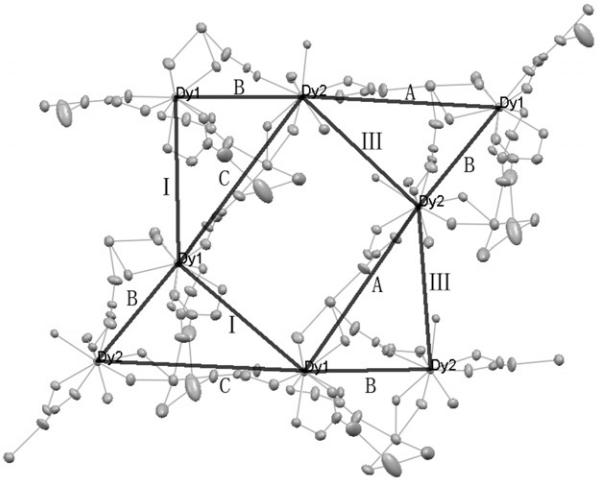

Figure 9. The structure of a layer in a unit cell of $Na_4[Dy^{III}(dtpa)(H_2O)]_2 \cdot 16H_2O$.

3.3.2. Molecular and crystal structures of $Na[Dy^{III}(edta)(H_2O)_3] \cdot 3.25H_2O$. The coordinate structures and crystal data of some analogues of $Na_4[Dy^{III}(edta)(H_2O)_3] \cdot 3.25H_2O$ [27] were reported by Nassimbeni *et al.* in 1979 [28]. However, comparing these analogues with $Na[Dy^{III}(edta)(H_2O)_3] \cdot 3.25H_2O$, there are some differences in molecular and crystal structures. The molecular structure of $Na[Dy^{III}(edta)(H_2O)_3] \cdot 3.25H_2O$ and its coordination polyhedron are shown in figures 11 and 12, respectively.

Figure 12 shows the molecular structure of the $[Dy^{III}(edta)(H_2O)_3]^-$ complex anion. The Dy^{III} ion is nine-coordinate by an edta ligand and three water molecules.

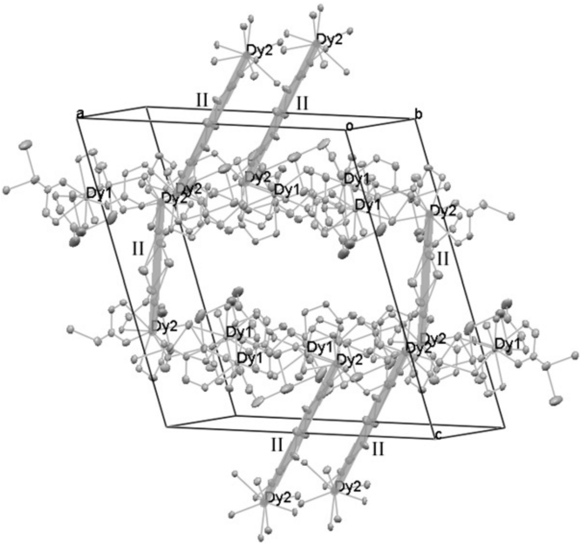

Figure 10. The structure between two layers in a unit cell of $Na_4[Dy^{III}(dtpa)(H_2O)]_2 \cdot 16H_2O$.

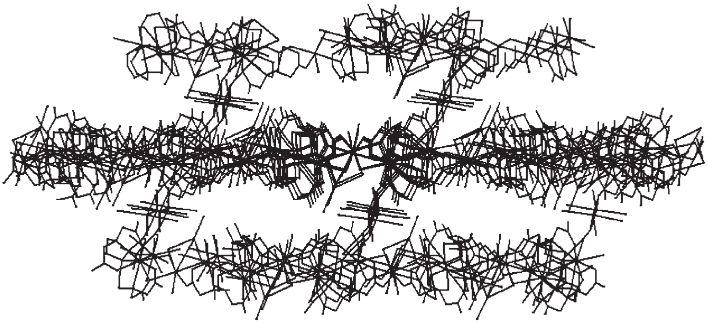

Figure 11. The 3-D crystal structure of $Na_4[Dy^{III}(dtpa)(H_2O)]_2 \cdot 16H_2O$ along the (0 1 0) direction.

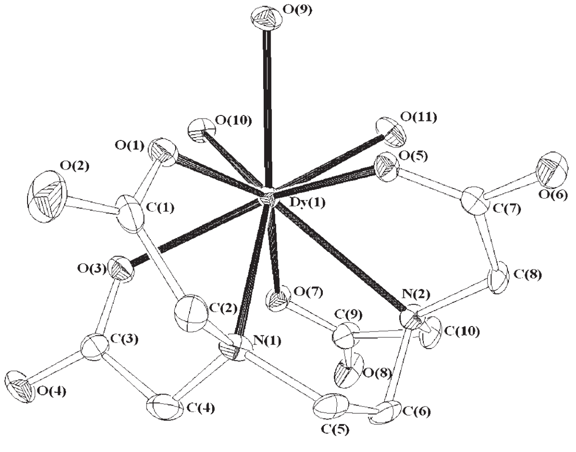

Figure 12. Molecular structure of the $[Dy^{III}(edta)(H_2O)_3]^-$ in $Na[Dy^{III}(edta)(H_2O)_3] \cdot 3.25H_2O$.

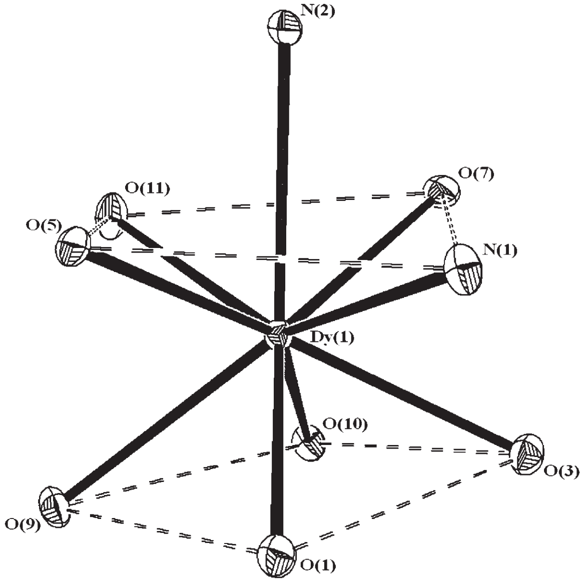

Figure 13. Coordination polyhedron around the Dy^{III} ion in $Na_4[Dy^{III}(edta)(H_2O)_3] \cdot 3.25H_2O$.

In the coordination atoms, three oxygen atoms come from water and two nitrogen atoms and four carboxyl oxygen atoms come from the edta ligand. The average bond length of Dy–O is 2.415(5) Å, which is shorter than the average bond length of Dy–N (2.649(4) Å) showing that Dy–O bonds are more stable than Dy–N bonds.

As shown in figure 13, the torsion angle is 8.46° between O(9)–O(1)–O(10) and O(3)–O(1)–O(10), so it is considered that the coordinating polyhedron of $Na[Dy^{III}(edta)(H_2O)_3] \cdot 3.25H_2O$ adopts a pseudo C_{4v} monocapped square antiprismatic conformation, a common conformation for nine-coordinate RE complexes with aminopolycarboxylic acid ligands. The top tetragon plane is composed of N(1), O(5), O(11) and O(7), and the bottom tetragon plane is composed of O(1), O(9), O(10) and O(3), which form a square antiprism. The capped position above the top tetragon plane is occupied by N(2). Because of the mutual repulsion between the top plane and the capped nitrogen atom, the bond length of Dy(1)–N(2) (2.673(6) Å) is the longest one of all the coordination bonds. Moreover, the distance between two planes becomes shorter than that of normal square antiprismatic conformation. Hence, the conformation of the coordination polyhedron is not standard C_{4v} monocapped square antiprism, but a slightly pseudo one.

The radius of the counter cation is still an important factor over the coordination structure. The radii of Na^+ and K^+ are relatively small, so they give the edta ligand more space to extend than the Cs^+ cation does in crystal lattices. As a result, there is space left for water molecules in coordination sphere. This is the reason why the coordination numbers of $K[Dy^{III}(edta)(H_2O)_3] \cdot 3.5H_2O$ and $Na[Dy^{III}(edta)(H_2O)_3] \cdot 3.25H_2O$ are both nine, whereas that of $Cs[Dy^{III}(edta)(H_2O)_2] \cdot 3H_2O$ is eight.

The $Na[Dy^{III}(edta)(H_2O)_3] \cdot 3.25H_2O$ crystallizes in the orthorhombic system with *Fdd*2 space group. The sodium cations are six coordinate by six oxygen atoms, as shown in figure 14. The bond lengths of Na–O range from 2.402(10) Å to 2.548(7) Å, and the average bond length is about 2.466(9) Å. Two come from two adjacent carboxyl groups,

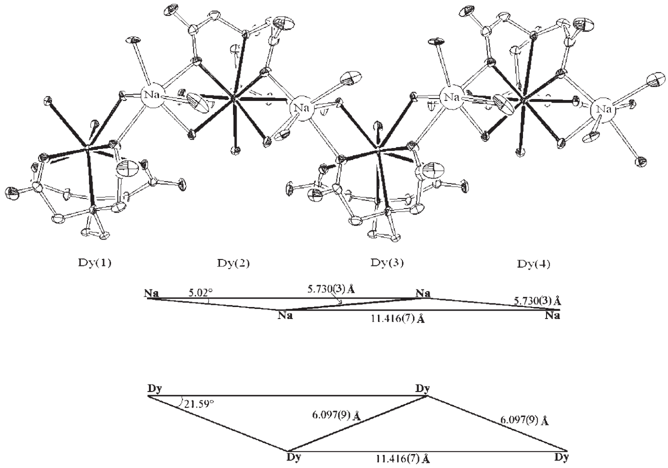

Figure 14. Infinite long zigzag type chain of Na[Dy^{III}(edta)(H$_2$O)$_3$] · 3.25H$_2$O.

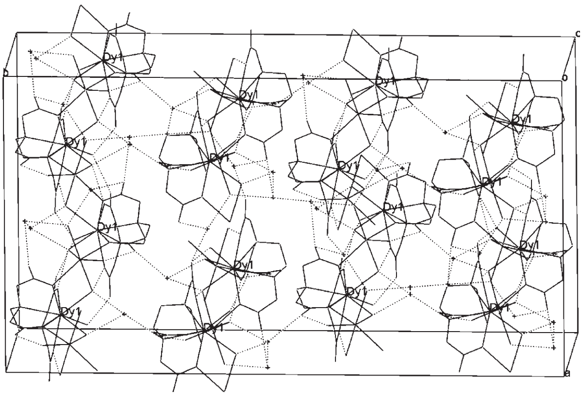

Figure 15. Arrangement of Na$_4$[Dy^{III}(edta)(H$_2$O)$_3$] · 3.25H$_2$O in a unit cell.

and other four come from the coordinate and crystal water molecules. Hence, the sodium cations bridge the coordination spheres yielding a 1-D zigzag type chain. All Dy^{III} ions in the same zigzag type chain are coplanar, and every four constitute a parallelogram. Two planes are parallel. In the parallelogram of Dy^{III} ions, two adjacent edges are 6.097(9) Å and 11.416(7) Å, respectively. The sharp angle between them is 21.59°. In the parallelogram of sodium cations, two adjacent edges are 5.730(3) Å and 11.416(7) Å, respectively. The sharp angle is 5.02°.

As shown in figure 15, there are six zigzag type chains through a unit cell. Between the coordination spheres, there are also intermolecular hydrogen bonds making the zigzag type chains more stable. In a unit cell, there are also many intermolecular hydrogen bonds keeping not only each zigzag type chain but the whole crystal structure more stable.

3.3.3. Molecular and crystal structures of Na$_3$[Dy^{III}(nta)$_2$(H$_2$O)] · 5.5H$_2$O. The crystal and molecular structure of some Dy-nta complexes were reported by

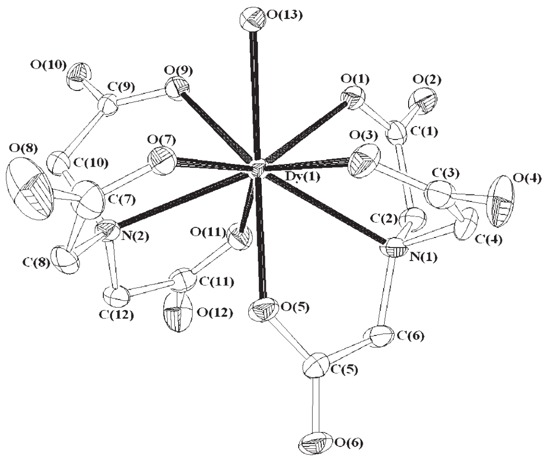

Figure 16. Molecular structure of the $[Dy^{III}(nta)_2(H_2O)]^{3-}$ in $Na_3[Dy^{III}(nta)_2(H_2O)] \cdot 5.5H_2O$.

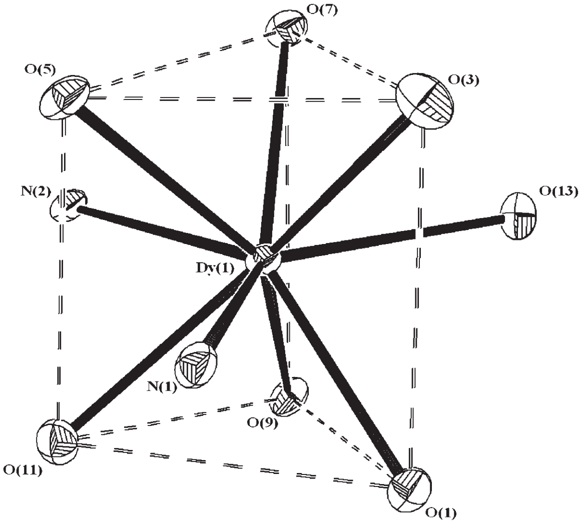

Figure 17. Coordination polyhedron around the Dy^{III} ion in $Na_3[Dy^{III}(nta)_2(H_2O)] \cdot 5.5H_2O$.

Martin and Jacobson [29]. For these complexes, the ratio of Dy^{III} ions to nta is 1 : 1. Whereas, in $Na_3[Dy^{III}(nta)_2(H_2O)] \cdot 5.5H_2O$, the ratio is 1 : 2. There are many other differences in the coordination number, the crystal and molecular structures.

Figure 16 exhibits the molecular structure of the $[Dy^{III}(nta)_2(H_2O)]^{3-}$ complex anion, in which the Dy^{III} ion is nine-coordinate with two nta ligands and one water. One oxygen atom, O(13), comes from water, and two nitrogen atoms and six carboxyl oxygen atoms come from two nta ligands. The average Dy–O bond length is 2.380(6) Å, while the average Dy–N bond length is 2.613(7) Å. The former is slightly shorter than the latter, which means that the Dy–O bonds are more stable than Dy–N bonds in $Na_3[Dy^{III}(nta)_2(H_2O)] \cdot 5.5H_2O$.

As shown in figure 17, the torsion angle is 26.75° between N(2)–O(5)–O(11) and N(1)–O(11)–O(5), near to 26.40°. So the coordination polyhedron of

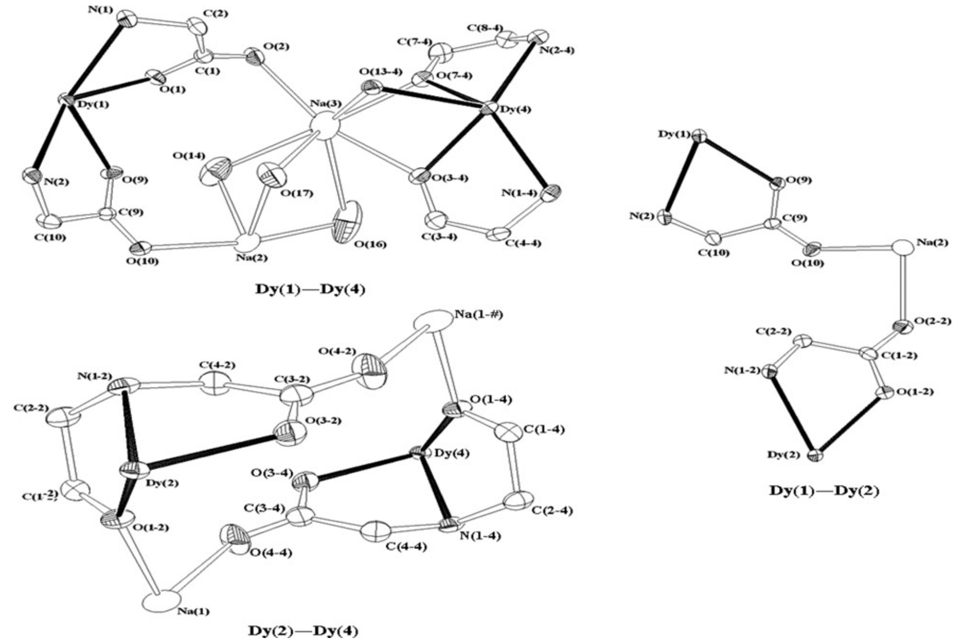

Figure 18. The different connecting modes between Dy^{III} ions in a unit cell of $Na_3[Dy^{III}(nta)_2(H_2O)] \cdot 5.5H_2O$.

$Na_3[Dy^{III}(nta)_2(H_2O)] \cdot 5.5H_2O$ adopts the slightly pseudo D_{3h} tricapped trigonal prismatic conformation, similar to other RE complexes with the nta ligand, such as $K_3[Sm^{III}(nta)_2(H_2O)] \cdot 6H_2O$, $Na_3[Gd^{III}(nta)_2(H_2O)] \cdot 5H_2O$, $K_3[Dy^{III}(nta)_2(H_2O)] \cdot 5H_2O$ [30] and $Na_3[Ho^{III}(nta)_2(H_2O)] \cdot 5H_2O$. The top plane is composed of O(3), O(5) and O(7), and the bottom plane is composed of O(1), O(11) and O(9), constituting a trigonal. Three capping positions are occupied by N(1), N(2) and O(13), respectively. The Dy^{III} ion and three capping atoms are approximately coplanar.

The influence from the radius of the counter cation still exists. The radii of Na^+ and K^+ are relatively small, so they give two nta ligands space in the crystal lattices. As a result, there is also space left for one water molecule in coordination sphere. The radius of the NH_4^+ cation is very big taking up space in the crystal lattices. This is the reason why the coordination numbers of $K_3[Dy^{III}(nta)_2(H_2O)] \cdot 5H_2O$ and $Na_3[Dy^{III}(nta)_2(H_2O)] \cdot 5.5H_2O$ are both nine, whereas that of $(NH_4)_3[Dy^{III}(nta)_2]$ is eight.

The $Na_3[Dy^{III}(nta)_2(H_2O)] \cdot 5.5H_2O$ crystallizes in the orthorhombic system with *Pccn* space group. In the crystal lattices, there are three kinds of sodium ions, Na(1), Na(2) and Na(3), with coordination number six. These Na^+ cations lie in the similar coordination environment as those of $Na_4[Dy^{III}(dtpa)(H_2O)]_2 \cdot 16H_2O$. The bond lengths of Na–O range from 2.309(8) Å to 2.994(15) Å, and the average bond length is 2.499(10) Å, connecting the many complex spheres.

As shown in figure 18, there are three types of bridging modes between two neighboring Dy^{III} ions, Dy(1)–Dy(2), Dy(1)–Dy(4) and Dy(2)–Dy(4), in $Na_3[Dy^{III}(nta)_2(H_2O)] \cdot 5.5H_2O$; each is provided with distinct crystal engineering functions. They could also be called "5+5" mode, because two extremities of the chain are both five-member rings.

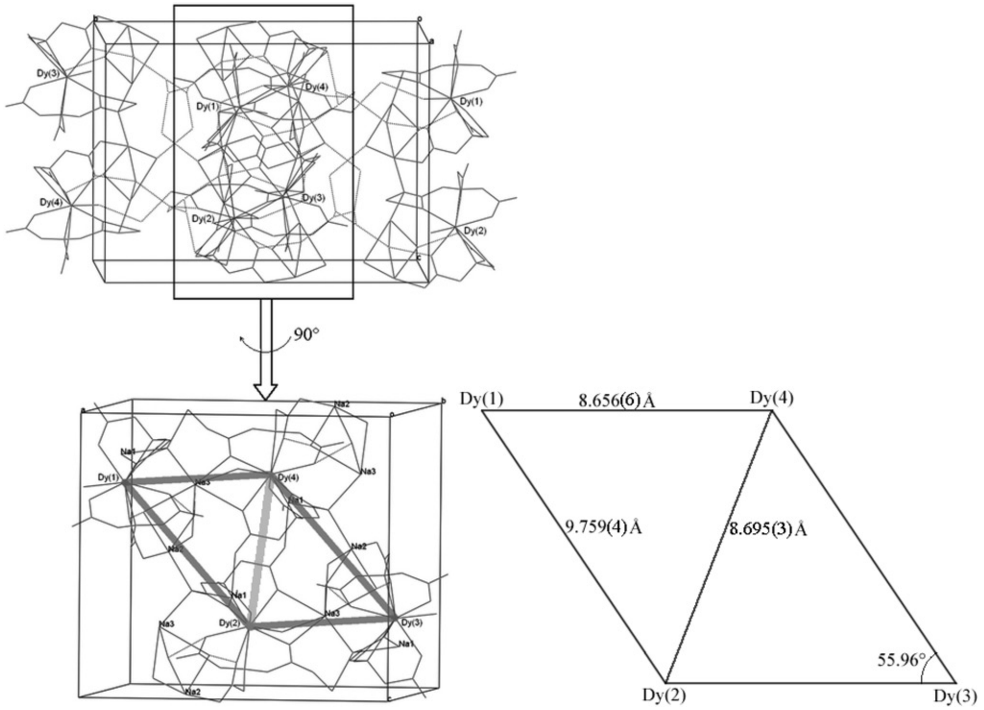

Figure 19. Arrangement of $Na_3[Dy^{III}(nta)_2(H_2O)] \cdot 5.5H_2O$ in a unit cell.

As shown in figure 19, four Dy ions are coplanar yielding a parallelogram. There is only one integrated parallelogram structure–unit and two halves in a unit cell of $Na_3[Dy^{III}(nta)_2(H_2O)] \cdot 5.5H_2O$. When the integrated one is turned left 90°, the parallelogram structure–unit could be appreciated clearly. The lengths of two parallel edges are the same, and the bridging coordination modes are the same too. The lengths of two adjacent edges are 8.656(6) Å and 9.759(4) Å, and the sharp angle is 55.96°. Along the diagonal Dy(2)–Dy(4) (8.695(3) Å), there are two bridging coordination chains, one above the parallelogram, and the other below. Between the parallelograms, there are many intermolecular hydrogen bonds keeping the crystal structure more stable.

4. Conclusion

Three RE complexes with different ligands (dtpa, edta and nta) but the same counter cation (Na^+) were synthesized. Their coordination numbers are all nine, but their coordination polyhedra and crystal structures are different. $Na_4[Dy^{III}(dtpa)(H_2O)]_2 \cdot 16H_2O$ with pseudo D_{3h} tricapped trigonal prismatic conformation possesses a 3-D layer-shaped structure; $Na[Dy^{III}(edta)(H_2O)_3] \cdot 3.25H_2O$ with the C_{4v} mono-capped square antiprismatic conformation possesses a 1-D zigzag type structure; $Na_3[Dy^{III}(nta)_2(H_2O)] \cdot 5.5H_2O$ with the D_{3h} tricapped trigonal prismatic conformation possesses a 2-D parallelogram structure. The collapsing temperatures of three complexes are 356°C for $Na_4[Dy^{III}(dtpa)(H_2O)]_2 \cdot 16H_2O$, 371°C for

$Na[Dy^{III}(edta)(H_2O)_3] \cdot 3.25H_2O$ and 387°C for $Na_3[Dy^{III}(nta)_2(H_2O)] \cdot 5.5H_2O$, respectively, proving that their crystal structures are very stable.

Supplementary material

CCDC 610103 ($Na_4[Dy^{III}(dtpa)(H_2O)]_2 \cdot 16H_2O$), CCDC 610104 ($Na[Dy^{III}(edta)(H_2O)_3] \cdot 3.25H_2O$) and CCDC 610105 ($Na_3[Dy^{III}(nta)_2(H_2O)] \cdot 5.5H_2O$) contain the supplementary crystallographic data for this article. These data can be obtained free of charge via www.ccdc.cam.ac.uk/data_request/cif, by e-mailing data_request@ccdc.cam.ac.uk, or by contacting the Cambridge Crystallographic Data Centre, 12 Union Road, Cambridge CB2 1EZ, UK; Fax: +44(0)1223-336033.

Acknowledgements

We thank Professor K. Miyoshi and T. Mizuta, Faculty of science, Hiroshima University, Japan, for instruction and Dr H.G. Wang, Central laboratory, Nankai University, China, for the single crystal X-ray structural determination. We also thank the software Mercury 1.4 (free), which helps us to analyze the crystal and molecular structures. These projects were supported by the National Natural Science Foundation of China (No. 20371023).

References

[1] C. Kremer, J. Torres, S. Dominguez, A. Mederos. *Coord. Chem. Rev.*, **249**, 567 (2005).
[2] P. Caravan, J.J. Ellison, T.J. McMurry. *Chem. Rev.*, **99**, 2293 (1999).
[3] A. Bianchi, L. Calabi, F. Corana, S. Fontana, P. Losi, A. Maiocchi, L. Paleari, B. Valtancoli. *Coord. Chem. Rev.*, **204**, 309 (2000).
[4] D.E. Reichert, J.S. Lewis, C.J. Anderson. *Coord. Chem. Rev.*, **184**, 3 (1999).
[5] M. Woods, Z. Kovacs, A.D. Sherry. *J. Supramol. Chem.*, **2**, 1 (2002).
[6] R.B. Lauffer. *Chem. Rev.*, **87**, 901 (1987).
[7] S.Z. Luo, M.F. Pu, J. Quao, Z.L. Liu, C.Y. Zhang, P.J. Zhao, Y.B. Fu, H.F. Deng. *J. Radioanal. Nucl. Chem.*, **160**, 443 (1992).
[8] W.A. Volkert, W.F. Goeckeler, G.J. Ehrhardt, A.R. Ketring. *J. Nucl. Med.*, **32**, 174 (1991).
[9] W.P. Li, D.S. Ma, C. Higginbotham, T. Hoffman, A.R. Ketring, C.S. Cutler, S.S. Jurisson. *Nucl. Med. Biol.*, **28**, 145 (2001).
[10] D. Parker, R.S. Dickins, H. Puschmann, C. Crossland, J.A.K. Howard. *Chem. Rev.*, **102**, 1977 (2002).
[11] A. Roig, R. Hettich, H.J. Schneider. *Inorg. Chem.*, **37**, 751 (1998).
[12] S.J. Oh, K.H. Song, D. Whang, K. Kim, T.H. Yoon, H. Moon, J.W. Park. *Inorg. Chem.*, **35**, 378 (1992).
[13] J.R. Morrow, L.A. Buttrey, V.M. Shelton, K.A. Berback. *J. Am. Chem. Soc.*, **114**, 1903 (1992).
[14] B.K. Takasaki, J. Chin. *J. Am. Chem. Soc.*, **115**, 9337 (1993).
[15] P.E. Jurek, A.M. Jurek, A.E. Martell. *Inorg. Chem.*, **39**, 1016 (2000).
[16] M. Komiyama, N. Takeda, H. Shigekawa. *Chem. Commun.*, **1443** (1999).
[17] P. Hurst, B.K. Takasaki, J. Chin. *J. Am. Chem. Soc.*, **118**, 9982 (1996).
[18] R. Wang, H. Liu, M.D. Carducci, T. Jin, C. Zheng, Z. Zheng. *Inorg. Chem.*, **40**, 2743 (2001).
[19] J. Wang, Y. Wang, X.D. Zhang, Z.H. Zhang, Y. Zhang, L.P. Kang, H. Li. *Russ. J. Coord. Chem.*, **58**, 921 (2005).
[20] J. Wang, J. Zhao, X.D. Zhang, J.Q. Gao. *Chin. Rare Metals*, **19**, 241 (2000).
[21] K. Nakamoto. *Infrared Spectra of Inorganic and Coordination Compounds*, 4th Edn, p. 231, John Wiley & Sons Inc., New York (1986).
[22] R.Y. Wang, J.R. Li, T.Z. Jin, G.X. Xu, Z.Y. Zhou, X.G. Zhou. *Polyhedron*, **16**, 1361 (1997).
[23] L.J. Guggenberger, E.L. Muetterties. *J. Am. Chem. Soc.*, **98**, 7221 (1976).
[24] Y. Inomata, T. Sunakawa, F.S. Howell. *J. Mol. Struct.*, **648**, 81 (2003).

[25] J. Wang, Y. Wang, X.D. Zhang, Z.H. Zhang, Y. Zhang, L.P. Kang, H. Li. *J. Coord. Chem.*, **58**, 921 (2004).

[26] N. Sakagami, J.I. Homma, T. Konno, K.I. Okamoto. *Acta Cryst.*, **C53**, 1378 (1997).

[27] L.R. Nassimbeni, M.R.W. Wright, J.C. van Niekerk, P.A. McCallum. *Acta Cryst.*, **B35**, 1341 (1979).

[28] N. Sakagami, Y. Yamada, T. Konno, K.I. Okamoto. *Inorg. Chim. Acta*, **288**, 7 (1999).

[29] L.L. Martin, R.A. Jacobson. *Inorg. Chem.*, **11**, 2789 (1971).

[30] J. Wang, G.R. Gao, Zh. H. Zhang, X. D. Zhang, X. Zh. Liu, Y.M. Kong, Y. Li. *J. Struct. Chem*, **C47**, 919 (2006).